Inorganic Chemistry

Article

pubs.acs.org/IC

Emission, Raman Spectroscopy, and Structural Characterization of Actinide Tetracyanometallates

Branson A. Maynard,[†] K. Sabrina Lynn,[†] Richard E. Sykora,[‡] and Anne E. V. Gorden[†,*]

[†]179 Chemistry, Department of Chemistry and Biochemistry, Auburn University, Auburn, Alabama 36830, United States

[‡]Department of Chemistry, University of South Alabama, Mobile, Alabama 36688, United States

Supporting Information

ABSTRACT: Three new compounds, $\{U_2(H_2O)_{10}(O)[Pt(CN)_4]_3\}\cdot 4H_2O$, $\{Th_2(H_2O)_{10}(OH)_2[Pd(CN)_4]_3\}\cdot 8H_2O$, and $\{(UO_2)_2(DMSO)_4(OH)_2[Ni(CN)_4]\}$, in the actinide tetracyanometallate, $An_x[M(CN)_4]_y$, class of compounds have been synthesized and characterized by confocal Raman spectroscopy and single crystal X-ray diffraction. These compounds contain unique structures illustrating dimeric actinide species. The absence of intense charge transfer emission in the visible range for $\{U_2(H_2O)_{10}(O)[Pt(CN)_4]_3\}\cdot 4H_2O$, as compared to the platinum starting material, is unusual because of the presence of pseudo-one-dimensional Pt···Pt chains in this compound. Confocal Raman spectroscopy of the cyanide stretching region provides insight into the binding domain (mono-, bi-, tri-, tetradentate) of the tetracyanometallates in these novel structures.

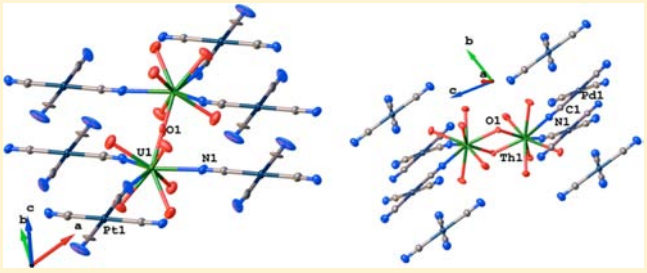

INTRODUCTION

Increasing the use of nuclear energy is one possible way to generate significant amounts of energy with low atmospheric emissions;[1] however, the extraction and use of uranium for nuclear fuel leads to many environmental concerns including long-term storage and remediation.[2−6] Uranium already plays a key role in our energy consumption. In the United States each year, 200 tons of uranium are required to fuel light-water reactors. Thorium is also being used increasingly in the design of new reactor systems, and thorium is estimated to be four times more abundant than uranium.[7] One strategy in the development of improved methods of uranium processing is to continue to further our understanding of actinide chemistry with detailed characterization of actinide coordination complexes.[7] For these reasons, the fundamental chemistry of actinide complexes has become of broad interest.[8−15]

Metal complex salts containing tetracyanoplatinate (TCPt) anions have been investigated for roughly 200 years.[16] Initial interest was in the differing colors of the complexes. The optical properties of these complexes could be altered by simply changing the cation in the solid state; the clear, colorless aqueous solutions were not as optically elegant.[16] These compounds have been reported in some alluring applications: they have been suggested for use in polymer electrolyte membrane fuel cells,[17] as catalyst precursors,[18] and in vapochromic sensing.[19] Prussian blue and Berlin blue analogs contain identical cyanide linkages between metal centers as the TCPt complexes. These cyano-bridged metal, M−N−C−M′, compounds have been shown to demonstrate intriguing magnetic behavior.[20−23]

In the mid 1980s, Gliemann and Yersin reviewed the properties of 36 solid state TCPt compounds known at that time, ranging from lithium as the lightest to thulium as the heaviest cation in the $Li_2[Pt(CN)_4]\cdot 4H_2O$ and $Tm_2[Pt(CN)_4]_3\cdot 21H_2O$ compounds, respectively.[16] This review outlined several structural features and parameters inherent to the TCPt class of compounds all relating to the quasi one-dimensional Pt chains observed in the solid-state structures. Quasi one-dimensional chains are formed in the solid state; platinophilic interactions may guide the square planar TCPt anions' tendency to stack. These parallel columns are thus thought to be responsible for the optical properties of this class of compounds.[16] The distance, *R*, between adjacent Pt atoms in these chains is considered critical in determining the characteristic emission properties. A simple equation has been derived to relate observed emission to the distance, *R*, between Pt atoms.[24] It has been noted that this distance can be altered by pressure, temperature, choice of cation, or magnetic fields.[16]

These early solid state TCPt compounds were noteworthy because of their striking optical features in the visible range.[16] Since this review was written more than 30 years ago, the TCPt class of compounds has been expanded.[24−27] The pseudo-one-dimensional Pt···Pt structural feature was allowed in the initial work, because the solvent used for these compounds, primarily, was H_2O. Since the early work in aqueous chemistry, several other polar solvents have successfully been used such as dimethyl sulfoxide, N,N-dimethyl acetamide, and N,N-dimethyl formamide;[25] however, solvation of the cation with larger solvent molecules tends to preclude the formation of the pseudo-one-dimensional Pt···Pt interactions and subsequent visible emission. Further extension of this class continued with

Received: November 9, 2012
Published: April 17, 2013

   dx.doi.org/10.1021/ic302459z | *Inorg. Chem.* 2013, 52, 4880−4889

Table 1

formula	$\{U_2(H_2O)_{10}(O)[Pt(CN)_4]_3\}\cdot 4H_2O$ (**U4**)	$\{Th_2(H_2O)_{10}(OH)_2[Pd(CN)_4]_3\}\cdot 8H_2O$ (**Th5**)	$\{(UO_2)_2(DMSO)_4(OH)_2[Ni(CN)_4]\}$ (**U6**)
formula mass	1613.57	1415.52	2094.72
color	emerald green	colorless	yellow
cryst syst	triclinic	triclinic	monoclinic
space group	$P\bar{1}$	$P\bar{1}$	$C2/c$
a (Å)	9.716 (4)	9.6141 (6)	21.5224(11)
b (Å)	9.823 (4)	9.9479 (6)	10.2531(5)
c (Å)	9.926 (4)	11.1360 (7)	13.3170(6)
α (deg)	74.191 (7)	73.7480 (10)	90
β (deg)	70.734 (7)	78.0950 (10)	111.9430(10)
γ (deg)	67.242 (7)	68.6530 (10)	90
V (Å^3)	813.2 (6)	945.82 (10)	2725.8(2)
Z	1	1	2
T (K)	183 (2)	183 (2)	183 (2)
λ (Å)	0.71073	0.71073	0.71073
μ (mm^{-1})	22.857	9.315	2.552
reflns collected	7998	9619	10040
unique reflns	3940	4604	3358
R_{int}	0.0582	0.0270	0.0292
R_1 [$I > 2\sigma(I)$]	0.0669	0.0282	0.0298
wR_2 (all data)	0.1681	0.0715	0.0746

the addition of aromatic ligands coordinating to the cationic metal center allowing for subsequent tuning of R in the TCPt chains. This also aided in the characterization of internal energy processes with the sensitization of weakly emitting lanthanide cations.[26] Work in this field after the Gliemann and Yersin review has focused on solvent and ancillary ligand effects and not incorporated actinide metal ions.[8]

We previously reported the first actinide tetracyanoplatinates to be structurally characterized using single crystal X-ray diffraction. For this report, we prepared and characterized three TCPt compounds: $Th(H_2O)_7[Pt(CN)_4]_2\cdot 10H_2O$ (**Th1**), $Th_2(H_2O)_{10}(OH)_2[Pt(CN)_4]_3\cdot 5H_2O$ (**Th2**), and $K_3[(UO_2)_2(OH)(Pt(CN)_4)_2]_2\cdot NO_3\cdot 1.5H_2O$ (**U3**) with Th^{4+} and UO_2^{2+} as the actinide cations.[8] It was remarkable that the thorium compounds, **Th1** and **Th2**, emitted while the uranyl compound, **U3**, lacked any observed emission.[8] Here, we report the synthesis, Raman spectroscopy, and structural characterization of three new compounds, $\{U_2(H_2O)_{10}(O)[Pt(CN)_4]_3\}\cdot 4H_2O$ (**U4**), $\{Th_2(H_2O)_{10}(OH)_2[Pd(CN)_4]_3\}\cdot 8H_2O$ (**Th5**), and $\{(UO_2)_2(DMSO)_4(OH)_2[Ni(CN)_4]\}$ (**U6**), of the actinide tetracyanometallate, $An_x[M(CN)_4]_y$, class of compounds. We compare these and include a discussion of the emission characteristics of **Th1** and **Th2**.

EXPERIMENTAL SECTION

Caution! *The $UO_2(NO_3)_2\cdot 6H_2O$ and UCl_4 used in this study contained depleted uranium. Standard precautions for handling radioactive materials or heavy metals, such as uranyl nitrate and thorium nitrate, were followed.*

Potassium tetracyanonickelate(II) hydrate (99.9%, Strem), potassium tetracyanopalladate(II) hydrate (98%, Strem), potassium tetracyanoplatinate(II) hydrate (98%, Strem), $UO_2(NO_3)_2\cdot 6H_2O$ (98%, J. T. Baker), $Th(NO_3)_4\cdot 6H_2O$ (99%, Fluka), and DMSO (99.9%, ACROS) were used as received without further purification. Deionized H_2O (7.2 MΩ cm) was obtained and used on site. UCl_4 was synthesized by the reaction of U_3O_8 with hexachloropropene reported by Hashimoto et al.[28]

$\{U_2(H_2O)_{10}(O)[Pt(CN)_4]_3\}\cdot 4H_2O$. Complex **U4** was synthesized in an inert atmosphere, employing Schlenk techniques to avoid the inclusion of O_2 into the system. Nitrogen gas was bubbled through H_2O contained in a Schlenk flask to exchange the dissolved O_2 gas with N_2 gas. The H_2O was cycled three times using a freeze–pump–thaw method to completely degas the H_2O. A portion of 0.0216 g (0.0569 mmol) of UCl_4 was weighed out inside an argon atmosphere glovebox and placed into a 200 mL Schlenk flask. Slightly less than 1 equivalent, 0.0207 g (0.0549 mmol) of $K_2[Pt(CN)_4]\cdot 3H_2O$, was weighed out and placed into a 50 mL Schlenk flask. With all three Schlenk flasks connected to the Schlenk line, a cannula was used to transfer the deoxygenated H_2O to the Schlenk flasks containing the starting materials. The solutions were stirred to allow the solids to dissolve. The $K_2[Pt(CN)_4]\cdot 3H_2O$ solution was then transferred by cannula into the Schlenk flask containing the UCl_4 solution. A small amount of precipitate that formed was removed by filtration. The mother liquor was placed in a −19 °C freezer where crystals suitable for single crystal X-ray diffraction (XRD) were observed to have formed after 6 days. Crystalline yield was not determined as the air sensitivity of the sample is significant and, therefore, cannot be accurately weighed on the bench. The presence of H_2O precluded sample manipulation or weighing in the Ar inert atmosphere glovebox.

$\{Th_2(H_2O)_{10}(OH)_2[Pd(CN)_4]_3\}\cdot 8H_2O$. Complex **Th5** was synthesized by weighing out 0.0200 g (0.0387 mmol) of $Th(NO_3)_4\cdot 6H_2O$ and 0.0146 g (0.0506 mmol) of $K_2[Pd(CN)_4]\cdot xH_2O$. Each was dissolved in a minimal amount of H_2O. The $K_2[Pd(CN)_4\cdot xH_2O$ solution was layered onto the $Th(NO_3)_4$ solution in a 5 mL test tube. The test tube was exposed to atmospheric conditions in a slow evaporation chamber where crystals suitable for single crystal XRD were observed to have formed after 27 days. Crystalline yield was 0.0148 g (67%).

$\{(UO_2)_2(DMSO)_4(OH)_2[Ni(CN)_4]\}$. Complex **U6** was synthesized by weighing out 0.0251 g (0.0500 mmol) of $UO_2(NO_3)_2\cdot 6H_2O$ and 0.0140 g (0.0581 mmol) of $K_2[Ni(CN)_4]\cdot xH_2O$. Each was dissolved in a minimal amount of H_2O. The $K_2[Ni(CN)_4\cdot xH_2O$ solution was layered onto the $UO_2(NO_3)_2\cdot H_2O$ solution in a 5 mL test tube. The test tube was exposed to atmospheric conditions where crystals suitable for single crystal XRD were observed to have formed after 32 days. Crystalline yield was 0.0118 g (45%).

X-Ray Crystallography. The X-ray diffraction data sets were collected at 183 K, on a Bruker SMART APEX CCD X-ray diffractometer unit using Mo Kα radiation, from crystals mounted in Paratone-N oil on glass fibers. SMART (v 5.624) was used for preliminary determination of cell constants and data collection control. Determination of integrated intensities and global cell refinement were performed with the Bruker SAINT software package using a narrow-frame integration algorithm. The program suite SHELXTL (v 5.1) was used for space group determination, structure solution, and refinement.[29] Refinement was performed against F^2 by weighted full-matrix

dx.doi.org/10.1021/ic302459z | Inorg. Chem. 2013, 52, 4880−4889

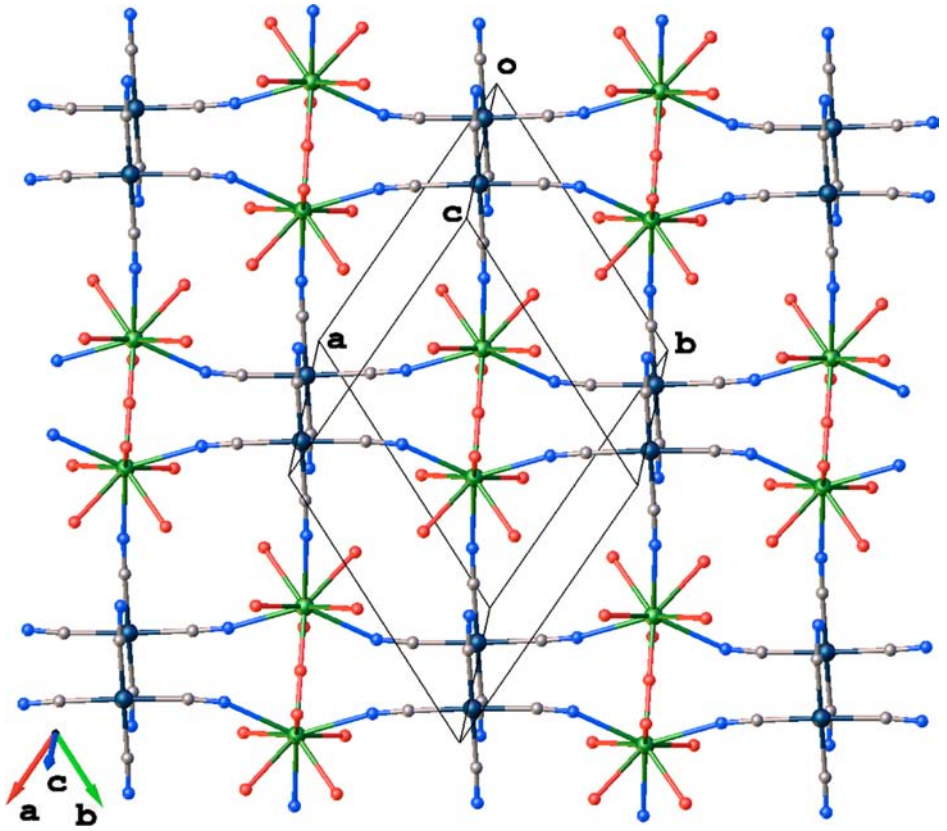

Figure 1. Projection of $\{U_2(H_2O)_{10}(O)[Pt(CN)_4]_3\}\cdot 4H_2O$ with lattice vectors shown. Hydration water molecules and hydrogens have been removed for clarity.

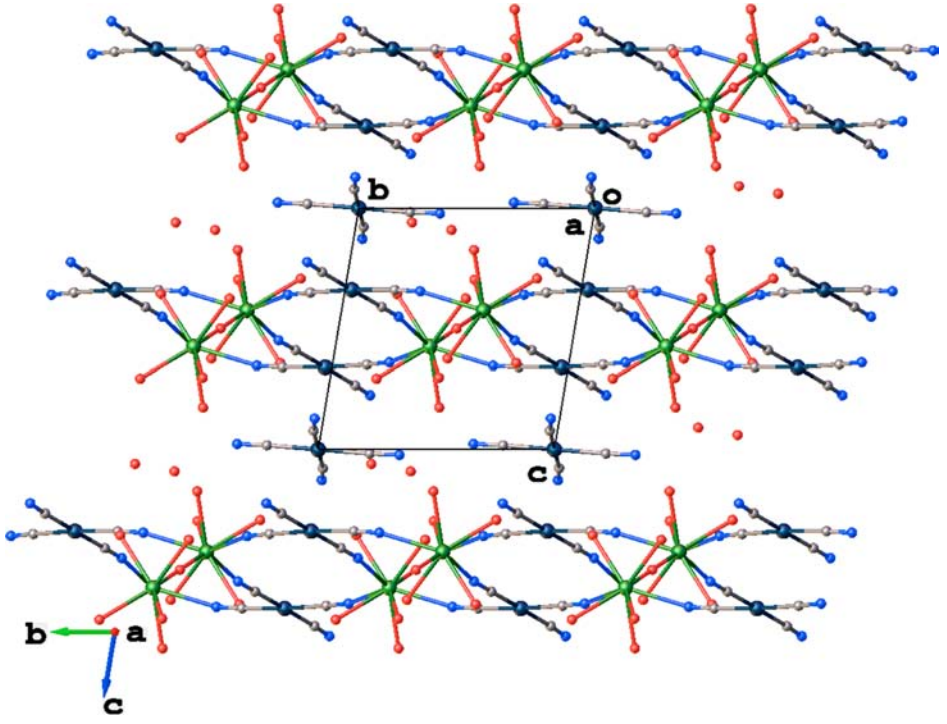

Figure 2. Packing diagram of **U4** showing the 2-D structural motif and the one-dimensional linear nonequidistant Pt···Pt chains along the *c* axis.

least-squares, and empirical absorption correction (SADABS) was applied. Hydrogen atoms for **U6** were found from the difference Fourier maps. Projections were generated in the Olex2.1−1 graphics program.[30] Table 1 contains key results of the X-ray experiments, and additional crystallographic information is included as Supporting Information.

Raman Spectroscopy. Raman spectroscopy was performed using the 514 nm line (20 mW) from an air-cooled argon ion laser (model

dx.doi.org/10.1021/ic302459z | *Inorg. Chem.* 2013, 52, 4880−4889

163-C42, Spectra-Physics Lasers, Inc.) as the excitation source. Raman spectra were collected and analyzed using a Renishaw inVia Raman microscope system. All of the spectroscopic experiments were conducted on neat crystalline samples held in sealed quartz capillary tubes at room temperature.

Photoluminescence Measurements. The photoluminescence spectra were collected using a Photon Technology International spectrometer (model QM-7/SE). The system uses a high intensity xenon source for excitation. Selection of excitation and emission wavelengths are conducted by means of computer controlled, autocalibrated "QuadraScopic" monochromators and are equipped with aberration corrected emission and excitation optics. Signal detection is accomplished with a photomultiplier tube detector (Hamamatsu model 928) that can work either in analog or digital (photon counting) modes. The instrument operation, data collection, and handling were all controlled using the FeliX32 fluorescence spectroscopic package. UV−vis data were acquired using a Craic Technologies 20/20 PV UV−visible microspectrophotometer. Spectra SI 18 through SI 24 were taken on a CRAIC 20/20 PV UV−visible microspectrophotometer. All of the spectroscopic experiments were conducted on neat crystalline samples held in sealed quartz capillary tubes at room temperature.

RESULTS

Crystallographic Description. *$\{U_2(H_2O)_{10}(O)[Pt(CN)_4]_3\}\cdot 4H_2O$ (**U4**).* The structure of **U4** has two-dimensional, bonding interactions, contains U(IV) as the actinide metal cation, and consists of $[U(H_2O)_5(O)(Pt(CN)_4)]$ units. Three tetracyanoplatinate anions and five water molecules coordinate the U(IV) metal center. One additional oxygen bridges two uranium sites to complete the coordination sphere as shown in Figure 1. The U(1)−O(1) bond distance at 2.0706(7) Å and the U−O−U bond angle of 180° corresponds well with another $U-O_{oxo}-U$ bridged species.[14] The overall coordination environment of the U(IV) site is nine, and this is best described geometrically as a tricapped trigonal prism. There are two distinct crystallographic tetracyanoplatinate anions in this structure. The structure is extended in two dimensions by the tetracyanoplatinate anions containing Pt1, which are tridentate and bridge three U sites, and the oxo bridge which links together two U sites as shown in Figure 1. The second tetracyanoplatinate anion containing Pt2 does not coordinate uranium but is present for charge balance and is involved in the formation of the pseudo-one-dimensional stacks as shown in Figure 2.

Each uranium center is coordinated by three tetracyanoplatinate anions; in turn each tridentate tetracyanoplatinate anion coordinates three U(IV) centers. An oxo bridge spans the U(IV) centers on the ladder structural features, thus forming the second dimension of the sheet. This forms a series of parallel ridges and furrows in conjunction with a macrostructure like a corrugated sheet. This structure does contain pseudo-one-dimensional tetracyanoplatinate chains, as shown in Figure 2, which is common with square planar cyanometallate complexes. In the pseudo-one-dimensional chains, there are two crystallographically independent Pt···Pt distances, 3.266(1) and 3.493(1) Å. These chains are described in the earlier literature as linear and nonequidistant with Pt atoms forming an x−y−y−x type structure. In this structure, x = a free $Pt(CN)_4^{2-}$ anion and y = a complexed $Pt(CN)_4^{2-}$ anion.[16] This type of chain structure is also described previously as linear nonequidistant, and it is often associated with partially oxidized systems.[16] The coordinating tetracyanoplatinate anions coordinate the uranium centers through three different U−N≡C bond angles, 172.3(15), 165.2(12), and 155.3(12)°. The $U-OH_2$ bonds range from 2.456(1) to 2.514(1) Å. The $U-O_{oxo}$ bond is 2.0706(7) Å, and the three U−N bonds range from 2.543(1) to 2.565(1) Å.

*$\{Th_2(H_2O)_{10}(OH)_2[Pd(CN)_4]_3\}\cdot 8H_2O$ (**Th5**).* The key feature of the structure of **Th5** is a series of one-dimensional chains of $\{Th_2(OH)_2(H_2O)(Pd(CN)_4)_3\}$. There is one crystallographically independent Th^{4+} center with a coordination number of nine, and it is best described geometrically as a tricapped trigonal prism. Three monodentate tetracyanopalladate anions and six oxygens coordinate the Th^{4+} metal center. Five of the coordinating oxygens are from water molecules, and the other two are from bridging hydroxides. Two hydroxide ions link the two Th^{4+} sites together and do not form bonds of equal length. The inversion symmetry is shown in two unique Th−OH bond distances of 2.337(3) and 2.371(3) Å. Two Th^{4+} ions sit 3.9858(4) Å apart from each other, which is a shorter distance than the sum of the van der Waals radii. The tetracyanopalladate anion bound to the Th^{4+} site extends the chain by binding to another asymmetric unit in a cis fashion. The pseudo-one-dimensional Pd···Pd chains are present and can be visualized in Figure 3. Again, chains like these are described in the earlier literature as linear and nonequidistant. The two crystallographically independent Pd···Pd distances are found at 3.2512(5) and 3.4960(9) Å. At first glance, the structures of **Th2** and **Th5** appear very similar, as both are described as one-dimensional.[8] Upon closer observation, the structure of **Th2** can be described as a polymeric structure consisting of $[-TCPt-Th-(OH)_2-Th-]^{+4}$ monomers. Inspection of **Th5** reveals that the polymeric structure is composed of $[-(OH)-Th-(TCPd)_2-Th-(OH)-]^{+2}$ monomers and is not isostructural with **Th2**.

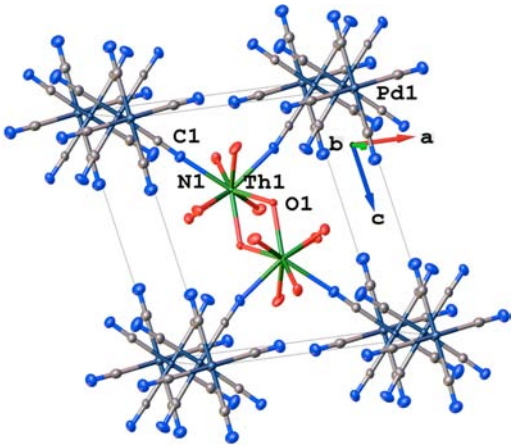

Figure 3. Projection of $\{Th_2(H_2O)_{10}(OH)_2[Pd(CN)_4]_3\}\cdot 8H_2O$ showing the pseudo-one-dimensional Pd···Pd interactions, along the *b* axis, with the unit cell superimposed. Thorium atoms are labeled in green, oxygen atoms in red, nitrogen atoms in blue, and palladium atoms in metallic blue.

*$\{(UO_2)_2(DMSO)_4(OH)_2[Ni(CN)_4]\}$ (**U6**).* The structure of $\{(UO_2)_2(DMSO)_4(OH)_2[Ni(CN)_4]\}$ (**U6**) has one-dimensional bonding interactions and consists of extended chains made up of $\{UO_2(DMSO)_4(OH)_2[Ni(CN)_4]\}$ units. There is one crystallographically independent UO_2^{2+} site. It has a coordination number of seven and is best described as a pentagonal bipyramid. Each UO_2^{2+} site is coordinated by six oxygen atoms and one tetracyanonickelate anion. Two oxygens are from the uranyl oxygen atoms and are found at distances of

dx.doi.org/10.1021/ic302459z | Inorg. Chem. 2013, 52, 4880−4889

1.776(4) and 1.779(4) Å from the metal ion. The second pair of coordinating oxygens are from the DMSO solvent molecule, and these are found at 2.380(4) and 2.391(4) Å. The third pair of coordinating oxygens are from the bridging hydroxides and have bond distances of 2.321(4) and 2.334(4) Å. One nitrogen from a cis bridging tetracyanonickelate anion also coordinates the UO_2^{2+} site. The structure is extended by two structural features along the one-dimensional chain: two bridging hydroxides connect uranyl sites, and the cis bridging tetracyanonickelate anion connects these uranyl sites extending the chain indefinitely. As compared to **Th2** and **Th5**, only a single TCNi unit bonds each UO_2^{2+} center. The polymeric structure of **U6** is clearly seen in Figure 4 consisting of

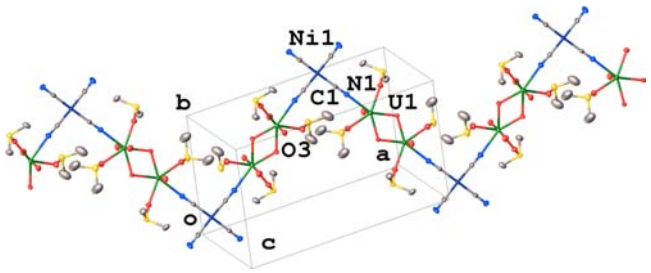

Figure 4. Extension of the one-dimensional structure of $\{(UO_2)_2(DMSO)_4(OH)_2[Ni(CN)_4]\}$ with the unit cell superimposed. Uranium atoms are labeled in green, oxygen atoms in red, nitrogen atoms in blue, and platinum atoms in blue metal. Hydrogen atoms are not shown for clarity.

$[-(OH)-UO_2-TCNi-UO_2-(OH)-]$ monomers. The monomer of **U6** resembles the monomer of **Th5**. In contrast, 3d metallophilicity is not observed, because the one-dimensional chains do not pack in such a way that Ni···Ni interactions are observed. The central reason for this is the small, hard 3d Ni^{2+} ions do not readily allow for metallophilic interactions. In addition, the inclusion of DMSO prohibits the stacking of TCNi, while by comparison, in **Th5**, the inclusion of H_2O allows for the TCPd anions to form the pseudo-one-dimensional chains.

Previous Results. We have reported three other actinide tetracyanoplatinate compounds in an earlier communication (**Th1**, **Th2**, and **U3**).[8] A brief overview of the structural characteristics of those complexes is presented here in an attempt to aid in the discussion of all six compounds (**Th1**, **Th2**, **U3**, **U4**, **Th5**, and **U6**). $Th(H_2O)_7[Pt(CN)_4]_2\cdot 10H_2O$ (**Th1**) is composed of monomers, $[Th(H_2O)_7(Pt(CN)_4)_2]$. The Th^{4+} metal center is bound by two monodentate tetracyanoplatinate anions. These monomers are not covalently bonded to another monomer; subsequently, the structural motif is best described as zero-dimensional. The formation of pseudo-one-dimensional Pt···Pt chains is observed from the stacking of the monomers. There are two Pt···Pt *R* values found at 3.3712(2) and 3.3515(2) Å. $Th_2(H_2O)_{10}(OH)_2[Pt(CN)_4]_3\cdot 5H_2O$ (**Th2**) is composed of $[Th_2(H_2O)_{10}(OH)_2(Pt(CN)_4)_3]$ chains and is best described as one-dimensional. Each Th^{4+} metal center is bound by two tetracyanoplatinate anions via two different modes of coordination, mono- and bidentate. The bidentate tetracyanoplatinate anion covalently extends the global structure in chains along one dimension. These chains pack in a way that formation of pseudo-one-dimensional Pt···Pt chains is observed. The Pt atoms in the pseudo-one-dimensional chains are spaced equidistant at 3.272(2) Å. The three-dimensional structure of **U3** is composed of $[UO_2(OH)(Pt(CN)_4)_4]$ units. Each UO_2^{2+} is bound by four tetradentate tetracyanoplatinate anions. The tetradentate tetracyanoplatinate anions extend the global structure in all three dimensions. The packing of this structure only allows the formation of Pt···Pt dimers, found at 3.221(1) Å.[8]

Excitation and Emission. Of the compounds we reported, both herein and previously,[8] the thorium compounds, **Th1** and **Th2**, have the most compelling absorption/emission properties. An example of the contrast upon excitation of the neat, solid samples with ambient or 365 nm radiation is shown in Figure 5. The excitation spectra of $K_2[Pt(CN)_4]\cdot 3H_2O$ can be characterized by the large band at 385 nm, which corresponds to a charge transfer state, on the TCPt anion, and the broadband emission feature at 425 nm is the relaxation of this excited charge transfer state.[31] Broad band excitation features are found in all three spectra; however, since it is known that the dominant form of thorium will be the Th^{4+} species, and thus all electrons will be spin paired in the electronic state, the excitation spectra do not originate from the Th^{4+} site.[32] This broad band excitation can be attributed to the charge transfer state on the $[Pt(CN)_4]^{2-}$ anion, which is what would be expected from the tetracyanoplatinate class of compounds featuring the Pt···Pt one-dimensional columns. What is stimulating are the low energy features found at 400, 425, and 440 nm in the excitation spectrum of **Th1** (Figure 6). It is likely that these features can be attributed to vibronic coupling as only one electronic transition is reported for Th^{4+} in this energy range, the 6d to 7s transition around 432 nm,[32] which does not match with these observed bands.

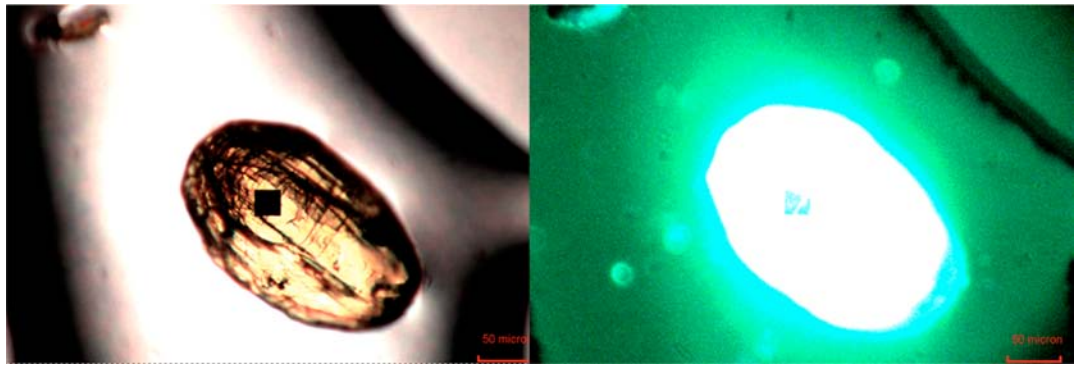

Figure 5. Single crystal sample of $Th(H_2O)_7[Pt(CN)_4]_2\cdot H_2O$. On the left the sample is viewed under a magnification of ×10. The same single crystal sample is viewed on the right under a magnification of ×10 and 365 nm excitation with the CRAIC microspectrophotometer.

dx.doi.org/10.1021/ic302459z | *Inorg. Chem.* 2013, 52, 4880−4889

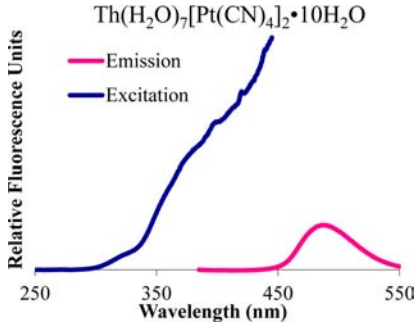

Figure 6. Excitation spectrum of $Th(H_2O)_7[Pt(CN)_4]_2 \cdot 10H_2O$ in blue monitored at a wavelength of 487 nm, and the emission spectrum in pink excited at 370 nm.

A correlation has been described in previous works that the separation of the Pt sites in the pseudo-one-dimensional chains directly corresponds to the emission wavelength.[24] It states that the shorter the distance, *R*, between the Pt···Pt sites within the chain, the lower the energy emission. The **Th1** and **Th2** compounds appear to follow this trend. The shortest Pt···Pt spacings in **Th1** and **Th2** are 3.3515(2) and 3.272(2) Å, respectively, with the λ_{max} of **Th2** red-shifted by ~50 nm as compared to the λ_{max} of **Th1**;[8] however, since Th^{4+} should not have excitation, and thus should not be emissive, the thorium sites of **Th1** and **Th2** seem to only function to adjust the Pt···Pt distance in these compounds. While there is a difference between the excitation profiles of the starting material, $K_2[Pt(CN)_4] \cdot 3H_2O$, as compared to **Th1** and **Th2**, the emission profiles can be characterized as the same and resultant of the relaxation of the charge transfer state.

Spectral features are also observed in the emission spectra (Figure 8) of **U4** at 435, 485, 544, 583, 611, and 707 nm. These

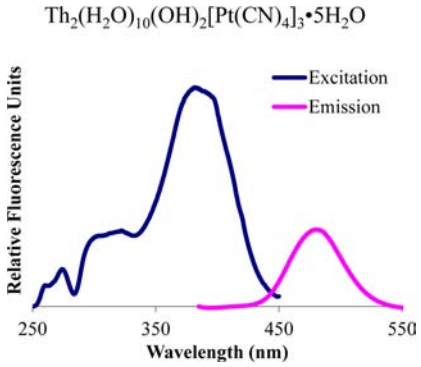

Figure 7. Excitation spectrum of $Th_2(H_2O)_{10}(OH)_2[Pt(CN)_4]_3 \cdot 5H_2O$ in blue monitored at a wavelength of 480 nm, and the emission spectrum in pink excited at 370 nm.

features are weaker in intensity and sharper, as can be surmised with emission originating from the U(IV) site;[33,34] as opposed to the charge transfer state on the TCPt anion that has broad intense emission features as seen in Figures 6, 7, and SI 16.

Raman Spectroscopy. The square planar tetracyanometallate anions are able to adopt several coordination modes (i.e., monodentate, trans- or cis-bridging, tri- and even tetradentate bridging), and uncoordinated tetracyanometallate anions can also be incorporated into the structure. For the simple potassium salts, A_{1g} and B_{1g} are the two CN vibrational modes expected in the cyanide stretching region between 2100 and 2300 cm^{-1}. The A_{1g} is more intense and has a larger Raman

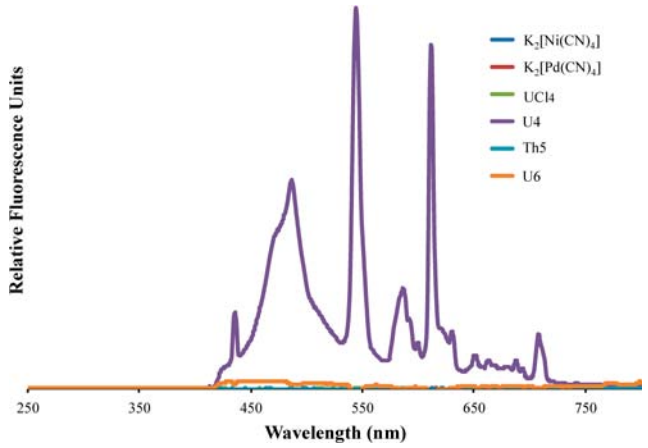

Figure 8. Emission spectra of **U4**, **Th5**, and **U6** in the visible region as compared to the cyanometallate starting materials.

shift as compared to the B_{1g}. Our values correlate well with data reported as seen in Table 2 (see also Figure 9 for Raman data

Table 2

assignment	$K_2[Ni(CN)_4] \cdot H_2O$	$K_2[Pd(CN)_4] \cdot H_2O$	$K_2[Pt(CN)_4] \cdot 3H_2O$
$\nu(CN)A_{1g}$	2132 (2132)[37]	2159 (2150)[36]	2164 (2168)[35]
$\nu(CN)B_{1g}$	2125 (2128)	2146 (2139)[36]	2143 (2149)[35]

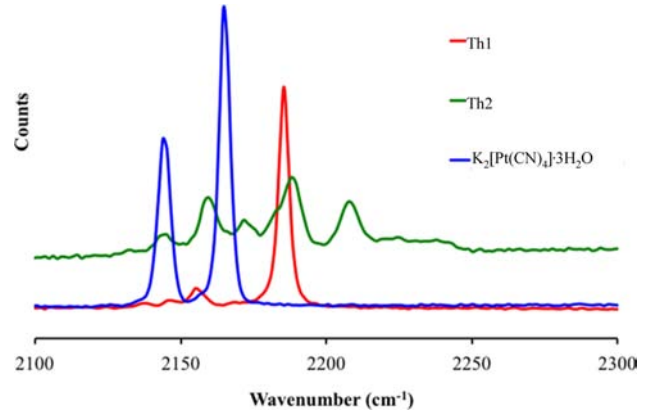

Figure 9. Raman data of $Th_x[Pt(CN)_4]_y$ compounds and the $K_2[Pt(CN)_4] \cdot 3H_2O$ starting material.

of $Th_x[Pt(CN)_4]_y$ compounds and the $K_2[Pt(CN)_4] \cdot 3H_2O$ starting material).[35−37] The assignment of the observed Raman shifts in our compounds is made easier if the square planar cyanometallates are considered as maintaining D_{4h} symmetry in the solid state. In this report, we have chosen to focus on the cyanide region; complete data of lower Raman shifts can be found in the Supporting Information.

Earlier, we described the first crystal structures from the actinide tetracyanoplatinate (AnTCPt) class of compounds.[8] Little has been reported previously about thorium compounds and identifiable features of Raman spectroscopy. Here, we wanted to further characterize these using the Raman features of these compounds. The compound $Th(H_2O)_7[Pt(CN)_4] \cdot 10H_2O$ (**Th1**) has two unique cyanide environments. One cyanide environment is only coordinated to the Pt center, and the other cyanide environment is coordinated to both the platinum and thorium metal center. As compared to the starting material, the peak height ratio of the A_{1g} and B_{1g} is

dx.doi.org/10.1021/ic302459z | Inorg. Chem. 2013, 52, 4880−4889

altered, and the Raman shifts are larger. The B_{1g} band blue shifts ~13 cm^{-1} while the A_{1g} band blue shifts ~20 cm^{-1}. Although the Th−N bonds in the $Th(H_2O)_7[Pt(CN)_4]\cdot 10H_2O$ compound (2.552(5) and 2.571(4) Å) are longer than other reported Th−N bonds,[38,39] the blue shift in the A_{1g} and B_{1g} bands of Figure 10 indicate electron density withdrawal from the N lone pair.[40,41]

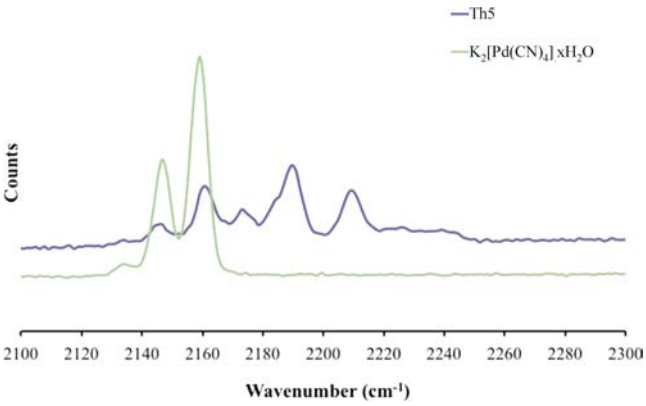

Figure 10. Raman spectra of $Th_2(OH)_2(H_2O)_{10}[Pd(CN)_4]_3\cdot 8H_2O$ and $K_2[Pd(CN)_4]\cdot xH_2O$.

In the second thorium cyanoplatinate compound, $Th_2(H_2O)_{10}(OH)_2[Pt(CN)_4]_3\cdot 5H_2O$ (**Th2**), there are two cyanide environments. One cyanide environment is coordinated to only the platinum center, while the other center is linked to both the platinum center and thorium center. This second environment is located trans to another such environment. As compared to $Th(H_2O)_7[Pt(CN)_4]\cdot 10H_2O$ (**Th1**), the $Th_2(H_2O)_{10}(OH)_2[Pt(CN)_4]_3\cdot 5H_2O$ (**Th2**) Raman spectra have more features, and the features are blue-shifted to a greater degree. The B_{1g} band appears at 2160 cm^{-1}; this peak blue shifts roughly ~17 cm^{-1} as compared to the starting material, $K_2[Pt(CN)_4]\cdot 3H_2O$. We believe the A_{1g} vibration has been blue-shifted ~26 cm^{-1} in agreement with the notion that the Th^{4+} withdraws electron density from the N lone pair. Three other spectral bands are seen at roughly 2145, 2173, and 2209 cm^{-1}, respectively.

In the first $Th[Pd(CN)_4]$ structure reported, $Th_2(OH)_2(H_2O)_{10}[Pd(CN)_4]_3\cdot 8H_2O$, like $Th_2(H_2O)_{10}(OH)_2[Pt(CN)_4]_3\cdot 5H_2O$, there are two cyanide environments. One cyanide environment is coordinated to only the palladium center, while the other environment is linked to both the palladium center and the thorium center. This second environment is located cis to another such environment. In good agreement with the $Th_2(H_2O)_{10}(OH)_2[Pt(CN)_4]_3\cdot 5H_2O$ compound, a total of five spectral features are seen (Figure 11) with the same peak trends. The B_{1g} band appears at 2162 cm^{-1}; this peak blue shifts roughly ~16 cm^{-1} as compared to the $K_2[Pt(CN)_4]$ starting material. We believe the A_{1g} vibration has been blue-shifted ~32 cm^{-1}, found at 2191 cm^{-1}, and this would be in agreement with the notion that the Th^{4+} withdraws electron density from the N lone pair. Three other spectral bands are seen at roughly 2147, 2174, and 2210 cm^{-1}, respectively.

In the first $U(IV)[Pt(CN)_4]$ structure reported, $(\{U_2(H_2O)_{10}(O)[Pt(CN)_4]_3\}\cdot 4H_2O)$ (**U6**), there are three cyanide environments. The first cyanide environment is coordinated to only the platinum atom. The second cyanide environment is coordinated to both the platinum atom and the uranium IV center and is trans to another identical environment, and the third cyanide environment is coordinated to both the platinum and the uranium IV center and is trans to the cyanide environment coordinated to only the platinum metal.

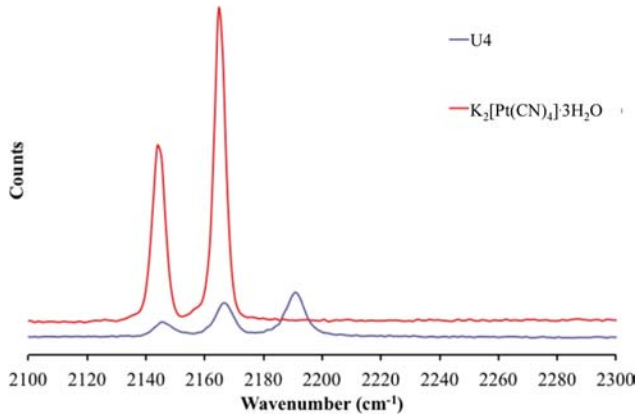

Figure 11. Raman spectrum of $\{U_2(H_2O)_{10}(O)][Pt(CN)_4]_3\}\cdot 4H_2O$.

DISCUSSION

Emission. An earlier paper reports the luminescent detection of metal ions including the limit of detection, 20 ppm, for the Th^{4+} metal ion.[42] The mode of characterization is described as ultraviolet examination with the emission characterization results for the white Th^{4+} precipitate given as green. The precipitate is formed under basic conditions by the addition of NH_3. The ThTCPt compounds that we reported formed greenish-yellow crystals and when irradiated with UV light gave a green emission (Figure 5). We attempted to grow ThTCPt crystals at higher pH, but the formation of $Th(OH)_4$ prevented this. For these reasons, we do not believe that the compounds we reported and the compounds from this much earlier report are the same.[42]

The lack of intense charge transfer emission in both the uranyl compound previously characterized, $K_3[(UO_2)_2(OH)(Pt(CN)_4)_2]_2\cdot NO_3\cdot 1.5H_2O$ (**U3**),[8] and the U(IV) compound reported here, $\{U_2(H_2O)_{10}(O)[Pt(CN)_4]_3\}\cdot 4H_2O$ (**U4**), is curious. The pseudo-one-dimensional Pt···Pt chains are not present in **U3**; only dimeric interactions are found at 3.2214(15) Å. Both the $K_2[Pt(CN)_4].3H_2O$ and $UO_2(NO_3)_2\cdot 6H_2O$ starting materials emit in the visible range, and it is odd that the product of these two materials is not emissive. Because **U3** lacks the long-range Pt···Pt interactions, the lack of intense charge transfer emission seen from **U4** may be of more interest as it contains the pseudo-one-dimension chains with *R* spacings of 3.266(1) and 3.493(1) Å. Further, any electronic energy transfer quenching should be forbidden as the TCPt does not change its multiplicity upon going from the ground state to the lowest excited state.[43]

The lack of emission in **Th5** and **U6** is expected. The Pd···Pd pseudo-one-dimensional structural feature is not linked to the same metal to ligand charge transfer visible emission as its 5d Pt···Pt counterpart. The formation of pseudo-one-dimensional Ni···Ni interactions in the TCNi class of compounds does not appear previously in the literature. The inclusion of DMSO may play a role in the lack of Ni···Ni interactions, but it is not solely responsible. The lack of these interactions is probably due to the smaller, harder nature of the 3d Ni atom as

dx.doi.org/10.1021/ic302459z | Inorg. Chem. 2013, 52, 4880−4889

Table 3

compound	B_{1g}			A_{1g}		mode
$Th(H_2O)_7[Pt(CN)_4]_2\cdot 10H_2O$	2146vw	2156w		2185s		monodentate
$Th_2(H_2O)_{10}(OH)_2[Pt(CN)_4]_3\cdot 5H_2O$	2141w	2160m	2173w	2189m	2209m	bidentate
$K_3[(UO_2)_2(OH)(Pt(CN)_4)_2]_2\cdot NO_3\cdot 1.5H_2O$		2143s		2164s		tetradentate
$\{U_2(H_2O)_{10}(O)[Pt(CN)_4]_3\}\cdot 4H_2O$	2146w	2167m		2191s		uncoordinated tridentate
$\{Th_2(OH)_2(H_2O)_{10}[Pd(CN)_4]_3\}\cdot 8H_2O$	2142w	2161m	2174w	2189s	2210m	uncoordinated bidentate
$\{(UO_2)_2(DMSO)_4(OH)_2[Ni(CN)_4]\}$		2138w		2161m		bidentate

compared to the larger, softer nature of the corresponding 4d and 5d Pd and Pt atoms.

Raman Spectroscopy. Few reports exist with Raman spectroscopy and structural data to accompany it involving TCNi interested in the mode of bridging of the TCNi anion.[44−48] Within these reports, only one structure is characterized as a cis or trans bridging structure,[44] and the rest involve the square planar TCNi that is either unbound or all nitrogens bind a metal and the D_{4h} symmetry is roughly preserved. In all of these reports, only single A_{1g} and B_{1g} vibrations are reported in the cyanide region (Table 3). We report all the peaks present in the νCN region of the Raman spectra and believe they correlate to the mode of binding of the d^8 tetracyanometallate, thus originating from the binding of the actinide metal. To our knowledge, there are no single crystal structural reports of TCPd or TCPt with Raman data to accompany it, making comparing assignments with other work a moot point. However, the blue shift of the Raman bands does correlate well with other cyanide bridged 4f and 5f and transition metal complexes.[40,41]

At first glance, the different actinide metal ions (Th^{4+}, U(IV), and UO_2^{VI}) appear to affect the cyanide region of the Raman data in different ways. As seen in the supplemental data, the UO_2^{2+} has little to no effect on shifting the vibrational modes in the cyanide region. It is interesting to note that when a $[Pt(CN)_4]^{2-}$ coordinates to a tetra positive uranium site, the cyanide region of the Raman spectrum displays a peak at 2192 cm^{-1}, roughly 28 cm^{-1} higher in energy than the A_{1g} vibration in the starting material. The largest difference occurs when a tetracyanometallate anion coordinates to a thorium. This is most likely a structural restriction, but this is hard to confirm, as an isostructural series has not been synthesized yet. In the three compounds containing U, as either UO_2^{2+} or U^{4+}, there are not any structural trends that correspond with the features seen in the Raman spectra. This makes the spectral features hard to elucidate.

Upon closer inspection, it seems that it is the binding modes (uncoordinated, mono-, bi-, tri-, and tetradentate), in which the tetracyanometallate anion is incorporated, that are responsible for the spectrum in the cyanide region. A monodentate tetracyanometallate, found in $Th(H_2O)_7[Pt(CN)_4]_2\cdot 10H_2O$, gives rise to three peaks; the two typical A_{1g} and B_{1g} peaks are still observed, but a significant third vibration also appears at lower frequency. When the tetracyanometallate coordinates the tetra positve thorium metal in a bridging, cis or trans, fashion as in $Th_2(H_2O)_{10}(OH)_2[Pt(CN)_4]_3\cdot 5H_2O$ and $\{Th_2(H_2O)_{10}(OH)_2[Pd(CN)_4]_3\}\cdot 8H_2O$, five peaks are seen in the cyanide region of the spectrum. Again, the typical A_{1g} and B_{1g} vibrations are found, but three other vibrations are observed at lower frequency. The tridentate bridging species $\{U_2(H_2O)_{10}(O)[Pt(CN)_4]_3\}\cdot 4H_2O$ gives three vibrations in the cyanide stretching region; again the $A1_g$ and $B1_g$ vibrations similar to the potassium salt are found, but a third vibration is found at lower frequency.

Of note in the compounds containing Th^{4+} is the similarity of the Raman features in the $Th_2(H_2O)_{10}(OH)_2[Pt(CN)_4]_3\cdot 5H_2O$ and $Th_2(OH)_2(H_2O)_{10}[Pd(CN)_4]_3\cdot 8H_2O$ structures. In the spectrum of each, there are five spectral features. Assigning the first two spectral features to the B_{1g} and A_{1g} vibrations, respectively, would indicate backbonding from the Th metal. Instead, the B_{1g} and A_{1g} vibrations are assigned to more blue-shifted spectral features in accordance with a bound metal withdrawing electron density from the N lone pair. The same spectral features are not observed in the $Th(H_2O)_7[Pt(CN)_4]\cdot 10H_2O$ compound (**Th1**). One possible explanation for this is the bridging features of the cyanometallate anion observed in the compounds. In both the $Th_2(H_2O)_{10}(OH)_2[Pt(CN)_4]_3\cdot 5H_2O$ (**Th2**) and $Th_2(OH)_2(H_2O)_{10}[Pd(CN)_4]_3\cdot 8H_2O$ (**Th5**) structures, the cyanometallates coordinate the Th^{4+} centers in a bidentate bridging fashion, and five spectral features are observed in the νCN region. This is in contrast to the $Th(H_2O)_7[Pt(CN)_4]\cdot 10H_2O$ (**Th1**) structure in which the coordinating cyanometallate only binds in a monodentate fashion, and three spectral features are observed in the νCN region.

The tetradentate species found in $K_3[(UO_2)_2(OH)(Pt(CN)_4)_2]_2\cdot NO_3\cdot 1.5H_2O$ shows only the A_{1g} and B_{1g} vibrations. Interesting is that the bridging cyanometallate species in $\{(UO_2)_2(DMSO)_4(OH)_2[Ni(CN)_4]\}$ show a similar spectrum as $K_2[Ni(CN)_4]\cdot xH_2O$, but the A_{1g} and B_{1g} vibrations are at lower frequency. The $\nu 1$ $(UO_2)^{2+}$ symmetric stretching vibration is observed at 826 cm^{-1} and correlates well with previous reports.[49,50] A weakness in characterizing these compounds by Raman spectroscopy alone is if the solid state structure contains more than one type of tetracyanometallate binding. With Raman data alone in the cyanide region of the spectrum you could only classify the tetracyanometallate mode of binding as tetradentate, monodentate−tridentate, and bidentate.

CONCLUSIONS

The ThTCPt compounds, **Th1** and **Th2**, are unique among the reported thorium literature, because we believe they are the first reported Th(IV) containing compounds to have both emission and structural work reported. The metal cation acts as a placeholder that tunes the *R* value between Pt centers in the pseudo-one-dimensional chains. **Th5** extends the set of reported, solid state thorium isocyanide complexes to a total of three. Mono-, bi-, and tridentate bridging TCMs, where M = Pt or Pd, have been shown in the solid state to give a fingerprint in the CN region of the Raman spectrum. Unfortunately, we were unable to synthesize an $An_x[Ni(CN)_4]_y$ analog in aqueous solution, and the DMSO incorporated into **U6** prohibits the formation of more peaks in the cyanide region of the Raman spectrum. Previous literature has only reported

dx.doi.org/10.1021/ic302459z | Inorg. Chem. 2013, 52, 4880−4889

two vibrations, A_{1g} and B_{1g}, in the 2000 cm^{-1} region. We report on one molecular unit and three bridging compounds that have more than two vibrations in this region of the Raman spectrum. This will provide valuable structural information when single crystal XRD analysis is not possible. Intensive computational analysis of these actinide cyanometallate systems is planned to better characterize the vibrational modes with more detail and affirm the presence or lack of orbital mixing of the metal and ligand in these actinide tetracyanometallate complexes.

■ ASSOCIATED CONTENT

Supporting Information

Additional data given in tables and figures. This material is available free of charge via the Internet at http://pubs.acs.org.

■ AUTHOR INFORMATION

Corresponding Author

*E-mail: gordeae@auburn.edu.

Notes

The authors declare no competing financial interest.

■ ACKNOWLEDGMENTS

Funding for the CRAIC UV−vis fluorescence microspectrophotometer was provided by a grant from the Auburn University Internal Grants Program to A.E.V.G. and the Department of Chemistry and Biochemistry. We gratefully acknowledge the Auburn University X-ray Diffraction Facility for assistance with the crystallographic characterization. Funds from the National Science Foundation (NSF-CAREER, CHE-0846680 to R.E.S.) supported this research. This work was supported in part by the Defense Threat Reduction Agency, Basic Research Award # HDTRA1-11-1-0044 to Auburn University.

■ REFERENCES

(1) *Nuclear Technology Review 2010*; International Atomic Energy (IAEA): Vienna, Austria, 2010.

(2) Albright, D.; Berkhout, F.; Walker, W. *Plutonium and Highly Enriched Uranium 1996: World Inventories, Capabilities, and Policies*; Stockholm International Peace Research Institute, Oxford University Press: New York, 1997.

(3) Gorden, A. E. V.; Xu, J. D.; Raymond, K. N.; Durbin, P. *Chem. Rev.* **2003**, *103*, 4207.

(4) *Nuclear Energy: Policies and Technology for the 21st Century*; Nuclear Energy Advisory Committee (NEAC), United States Department of Energy: Washington, DC, 2008; p 31.

(5) *Annual Energy Review 2010*; United States Energy Information Administration, U. S. Department of Energy: Washington, DC, 2011.

(6) *The Future of the Nuclear Fuel Cycle: An Interdisciplinary Study*; MIT Nuclear Fuel Cycle Study Advisory Committee, Massachussetts Institute of Technology (MIT): Cambridge, MA, 2011.

(7) Britt, P.; Forsberg, C.; Herring, S. *Technology and Applied R&D Needs for Nuclear Fuel Resources*; Department of Energy, Office of Nuclear Energy: Washington, DC, 2010; p 52.

(8) Maynard, B. A.; Sykora, R. E.; Mague, J. T.; Gorden, A. E. *Chem. Commun.* **2010**, *46*, 4944.

(9) Cantat, T.; Graves, C. R.; Scott, B. L.; Kiplinger, J. L. *Angew. Chem., Int. Ed.* **2009**, *48*, 3681.

(10) DeVore, M. A.; Gorden, A. E. V. *Polyhedron* **2012**, *42*, 271.

(11) Melfi, P. J.; Kim, S. K.; Lee, J. T.; Bolze, F.; Seidel, D.; Lynch, V. M.; Veauthier, J. M.; Gaunt, A. J.; Neu, M. P.; Ou, Z.; Kadish, K. M.; Fukuzumi, S.; Ohkubo, K.; Sessler, J. L. *Inorg. Chem.* **2007**, *46*, 5143.

(12) Pasquale, S.; Sattin, S.; Escudero-Adan, E. C.; Martinez-Belmonte, M.; de, M. J. *Nat. Commun.* **2012**, *3*, 1793/1.

(13) Schnaars, D. D.; Batista, E. R.; Gaunt, A. J.; Hayton, T. W.; May, I.; Reilly, S. D.; Scott, B. L.; Wu, G. *Chem. Commun.* **2011**, *47*, 7647.

(14) Daly, S. R.; Ephritikhine, M.; Girolami, G. S. *Polyhedron* **2012**, *33*, 41.

(15) Monreal, M. J.; Thomson, R. K.; Cantat, T.; Travia, N. E.; Scott, B. L.; Kiplinger, J. L. *Organometallics* **2011**, *30*, 2031.

(16) Gliemann, G.; Yersin, H. *Struct. Bonding (Berlin)* **1985**, *62*, 87.

(17) Di, N. V.; Negro, E.; Vezzu, K.; Toniolo, L.; Pace, G. *Electrochim. Acta* **2011**, *57*, 257.

(18) Ding, E.; Sturgeon, M. R.; Rath, A.; Chen, X.; Keane, M. A.; Shore, S. G. *Inorg. Chem.* **2009**, *48*, 325.

(19) Cich, M. J.; Hill, I. M.; Lackner, A. D.; Martinez, R. J.; Ruthenburg, T. C.; Takeshita, Y.; Young, A. J.; Drew, S. M.; Buss, C. E.; Mann, K. R. *Sens. Actuators, B* **2010**, *B149*, 199.

(20) Perrier, M.; Long, J.; Paz, F. A. A.; Guari, Y.; Larionova, J. *Inorg. Chem.* **2012**, *51*, 6425.

(21) Dumont, M. F.; Knowles, E. S.; Guiet, A.; Pajerowski, D. M.; Gomez, A.; Kycia, S. W.; Meisel, M. W.; Talham, D. R. *Inorg. Chem.* **2011**, *50*, 4295.

(22) Le, B. R.; Tsunobuchi, Y.; Mathoniere, C.; Tokoro, H.; Ohkoshi, S.-i.; Ould-Moussa, N.; Molnar, G.; Bousseksou, A.; Letard, J.-F. *Inorg. Chem.* **2012**, *51*, 2852.

(23) Mizuno, Y.; Okubo, M.; Kagesawa, K.; Asakura, D.; Kudo, T.; Zhou, H.; Oh-ishi, K.; Okazawa, A.; Kojima, N. *Inorg. Chem.* Ahead of print.

(24) Loosli, A.; Wermuth, M.; Gudel, H. U.; Capelli, S.; Hauser, J.; Burgi, H. B. *Inorg. Chem.* **2000**, *39*, 2289.

(25) Du, B.; Meyers, E. A.; Shore, S. G. *Inorg. Chem.* **2001**, *40*, 4353.

(26) Maynard, B. A.; Kalachnikova, K.; Whitehead, K.; Assefa, Z.; Sykora, R. E. *Inorg. Chem.* **2008**, *47*, 1895.

(27) Maynard, B. A.; Sykora, R. E. *Acta Crystallogr., Sect. E: Struct. Rep. Online* **2008**, *E64*, m138.

(28) Ito, K.; Kanno, T.; Hashimoto, H. *Nippon Genshiryoku Gakkaishi* **1974**, *16*, 544.

(29) Sheldrick, G. M. *Acta Crystallogr., Sect. A: Found. Crystallogr.* **2008**, *A64*, 112.

(30) Dolomanov, O. V.; Bourhis, L. J.; Gildea, R. J.; Howard, J. A. K.; Puschmann, H. *J. Appl. Crystallogr.* **2009**, *42*, 339.

(31) Cowman, C. D.; Gray, H. B. *Inorg. Chem.* **1976**, *15*, 2823.

(32) *The Chemistry of the Actinide and Transuranic Elements*, 3rd ed.; Morss, L., Edelstein, N. M., Fuger, J., Katz, J. J., Eds.; Springer: Dordrecht, The Netherlands, 2006.

(33) Simoni, E.; Hubert, S.; Genet, M. *J. Phys. (Paris)* **1988**, *49*, 1425.

(34) Godbole, S. V.; Page, A. G.; Sangeesta; Sabharwal, S. C.; Gesland, J. Y.; Sastry, M. D. *J. Lumin.* **2001**, *93*, 213.

(35) Benner, R. E.; Von, R. K. U.; Lee, K. C.; Owen, J. F.; Chang, R. K.; Laube, B. L. *Chem. Phys. Lett.* **1983**, *96*, 65.

(36) Gans, P.; Gill, J. B.; Johnson, L. H. *J. Chem. Soc., Dalton Trans.* **1993**, 345.

(37) McCullough, R. L.; Jones, L. H.; Crosby, G. A. *Spectrochim. Acta* **1960**, *16*, 929.

(38) Pool, J. A.; Scott, B. L.; Kiplinger, J. L. *Chem. Commun.* **2005**, 2591.

(39) Schelter, E. J.; Morris, D. E.; Scott, B. L.; Kiplinger, J. L. *Chem. Commun.* **2007**, 1029.

(40) Assefa, Z.; Haire, R. G.; Sykora, R. E. *J. Solid State Chem.* **2008**, *181*, 382.

(41) Assefa, Z.; Kalachnikova, K.; Haire, R. G.; Sykora, R. E. *J. Solid State Chem.* **2007**, *180*, 3121.

(42) Capelin, B. C.; Ingram, G. *Talanta* **1970**, *17*, 187.

(43) Matsushi., R.; Fujimori, H.; Sakuraba, S. *J. Chem. Soc., Faraday Trans.* **1974**, *70*, 1702.

(44) Kuerkcueoglu, G. S.; Hoekelek, T.; Aksel, M.; Yesilel, O. Z.; Dal, H. *J. Inorg. Organomet. Polym. Mater.* **2011**, *21*, 602.

(45) Kurkcuoglu, G. S.; Yesilel, O. Z.; Kavlak, I.; Buyukgungor, O. *Struct. Chem.* **2008**, *19*, 879.

(46) Agusti, G.; Cobo, S.; Gaspar, A. B.; Molnar, G.; Moussa, N. O.; Szilagyi, P. A.; Palfi, V.; Vieu, C.; Munoz, M. C.; Real, J. A.; Bousseksou, A. *Chem. Mater.* **2008**, *20*, 6721.

(47) Lemus-Santana, A. A.; Rodriguez-Hernandez, J.; del Castillo, L. F.; Basterrechea, M.; Reguera, E. *J. Solid State Chem.* **2009**, *182*, 757.
(48) Kurkcuoglu, G. S.; Yesilel, O. Z.; Cayli, I.; Buyukgungor, O. *J. Mol. Struct.* **2011**, *994*, 39.
(49) Frost, R. L; Cejka, J.; Weier, M. L.; Martens, W. *J. Raman Spectrosc.* **2006**, *37*, 538.
(50) Frost, R. L; Cejka, J.; Dickfos, M. J. *J. Raman Spectrosc.* **2009**, *40*, 38.